Electron Cyclotron Emission from a Tokamak Plasma: Experiment and Theory

A. E. Costley,* R. J. Hastie, J. W. M. Paul, and J. Chamberlain*
United Kingdom Atomic Energy Authority Research Group, Culham Laboratory, Abingdon, Berkshire, United Kingdom
(Received 24 June 1974)

We present the first measurements of the power, polarization, and frequency spectrum of the electron cyclotron emission from a tokamak plasma. The radiation is not polarized, does not have the previously predicted spectrum, and under certain circumstances is an order of magnitude above the predicted power level. We interpret the results in terms of a scrambling of polarization on reflection within the torus and in terms of the emission from suprathermal electrons.

Electron cyclotron emission from hot toroidal plasmas is currently of importance in fusion research. It is anticipated that it could constitute a significant power loss in a reactor[1,2] and that a measurement of it could be an informative plasma-diagnostic technique.[3] In this Letter we present measurements of the electron cyclotron emission (occurring at millimeter wavelengths) from the hot plasma of a tokamak device.

The plasma investigated is produced by the CLEO tokamak.[4] It has a toroidal flux density $B_\varphi \leq 2.0$ T, a mean electron density $n_e \sim 2\times10^{19}$ m^{-3}, a central electron temperature $T_{e0} \sim 300$ eV, a central ion temperature $T_{i0} \sim 200$ eV, a major radius $R_0 = 0.9$ m, a minor radius $a_0 = 0.18$ m, and duration up to 180 msec.

Emission measurements.—These were made by observing the plasma along a major radius through a wedge-shaped window of crystal quartz (Z cut). Radiation from the plasma was directed into a two-beam polarization-type interferometer.[5] The path difference (x) within this was scanned in 10 msec over the range $-1 < x < 9$ mm by oscillation of one of the interferometer mirrors, and the resulting interference patterns (Fig. 1) were detected with a Putley indium antimonide detector. (The spectrally integrated emission was also detected for reference purposes.) Subsequent Fourier transformation of the interference patterns and calibration of the apparatus yielded the emission spectra.

In the calibration the time dependence of the path difference was measured by using an HCN laser ($\lambda = 337$ μm) and the absolute power response of the interferometer-detector arrangement was determined with a dc mercury arc lamp. Such lamps have been shown previously[6] to radiate approximately as a black body with a radiation temperature of 3000 K.

The emission spectrum from a typical tokamak shot is shown in Fig. 2 (curve *a*). The resolution in the spectrum is determined by the total scan x_m used in the Fourier transform, $R = cx_m^{-1}$, and in this case is 37.5 GHz. As expected, emission peaks occur at the cyclotron harmonics ($n\omega_{ce}$) $n = 2$, 3, and 4 for the magnetic field B_0 at the center of the plasma. The emission at $n = 1$ (i.e., I_1) could not be deduced by the normal procedure since the calibration system was insensitive in this region. However, from the known responsivity of the Putley detector an upper limit can be placed on I_1 as in Fig. 2.

By combining data recorded on two identical tokamak shots, spectra with an improved resolution of 25 GHz were obtained (Fig. 2, curve *b*). A mirror in the fixed arm of the interferometer was displaced between the two shots so that adjacent parts of the interference patterns were scanned, and composite interference patterns were constructed and transformed.

Variation of the tokamak conditions revealed a clear correlation between the level and spectrum

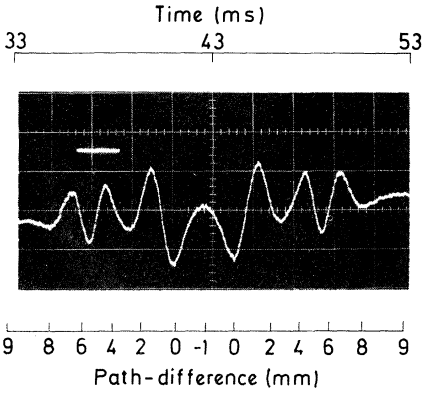

FIG. 1. Signal from the interferometer showing two scans of the interference pattern, traversed in opposite directions. (Time is from initiation of discharge.)

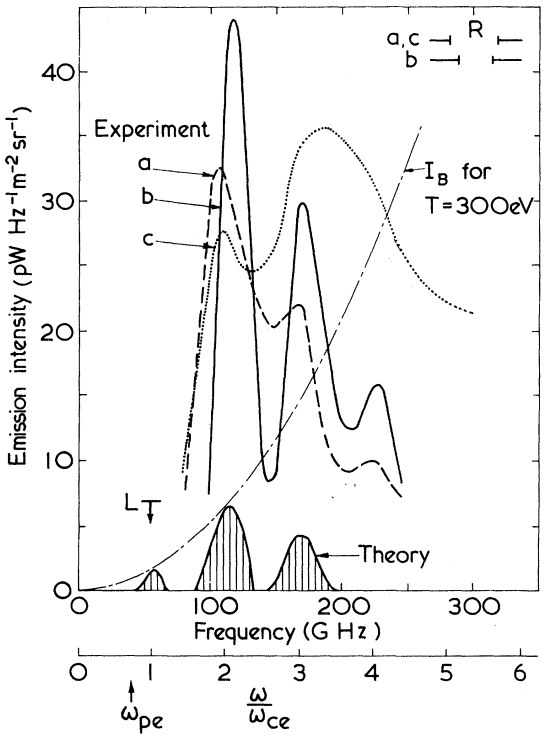

FIG. 2. Emission spectra. Experiment: curve *a*, single scan from Fig. 1; curve *b*, composite scan; curve *c*, single scan but with appreciable runaway (*L* is the limit of detectability). Theoretical: prediction for polarized emission (extraordinary mode, vertical hatching). ω_{pe} is plasma frequency.

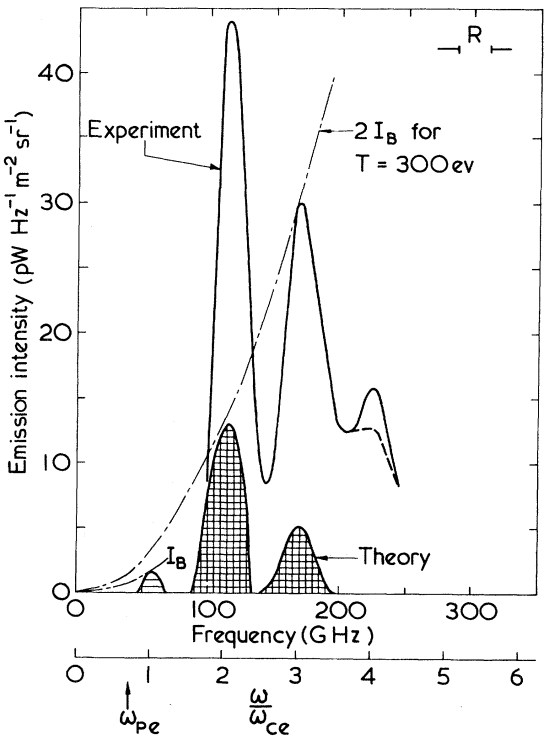

FIG. 3. Emission spectra. Experiment: composite scan (effect of smoothed calibration at $n=4$, dashed line). Theoretical: prediction with polarization scrambling (ordinary mode, horizontal hatching; and unpolarized, cross hatching).

of the emission (e.g., Fig. 2, curve *c*), and the level of hard x-ray emission. (Note that the latter is an indication of the presence of high-energy runaway electrons.) Under conditions of relatively intense x-ray emission the spectrally unresolved monitor showed an increase of up to an order of magnitude in emitted power.

The uncertainties in the measurement method are such that the relative shape and frequency position of the spectral features are reliable to about ±10%, and that the absolute level of the spectra is reliable to about an order of magnitude (i.e., factor of 3 either way). The latter uncertainty arises mainly from the need to use different optical and electronic systems for the calibration and the plasma measurements. The emission in the region of $4\omega_{ce}$ is subject to a ±20% uncertainty because of the presence of a small unidentified feature at about 225 GHz in the calibration data. The effect of smoothing this feature is shown in Fig. 3.

Polarization measurements.—The orientation of a wire polarizer in the interferometer was changed between discharges and the resulting interference patterns were recorded. Since the transformed spectra were the same to within the discharge reproducibility limits (±10%), the detected radiation was unpolarized (to within this uncertainty) at all frequencies in the region examined.

In a separate experiment an optical system of smaller *étendue*, which excluded radiation reflected in the torus side arm, was used, and spectrally integrated signals were recorded. Since these were independent of the orientation of a wire polarizer mounted in the optical system, we conclude that the radiation that crossed the plasma-vacuum boundary was unpolarized.

In an effort to understand this lack of polarization we measured the depolarizing effect of multiple reflections within the stainless-steel torus. With no plasma present the torus was irradiated with a polarized beam of 2-mm-wavelength radiation and the polarization state of the radiation emanating from several radial ports was determined. While radiation from a port immediately

adjacent to the entrance port ($\varphi = 20°$) was partially polarized that from other ports with $\varphi \geq 90°$ was less than $\pm 10\%$ polarized, demonstrating that multiple reflections within the torus can depolarize the radiation.

Theory for polarized emission.—We consider the cyclotron emission from a toroidal plasma in the direction of the major radius[2,3] (nonrelativistic limit for $T_e \sim 300$ eV). The intensity[7] $I_g(\omega)$ in each mode (extraordinary, $g = e$; ordinary, $g = o$) is given by[8]

$$I_g = I_B \frac{1 - \exp(-\int \alpha_g ds)}{1 - r \exp(-\int \alpha_g ds)}, \quad (1)$$

where $\alpha_g(\omega)$ is the absorption coefficient of the plasma, $I_B = \omega^2 k T_e / 8\pi^3 c^2$ is the black-body intensity for a single mode, and $r = r(\omega)$ is the reflection coefficient of the metal wall bounding the plasma. The spatial contributions are integrated across the toroidal profile with arbitrary $n_e(s)$, $T_e(s)$, and defined $B(s) = B_0(1 - s/R_0)$, $|s| \geq a_0$. For each ω and harmonic n, the resonance $\omega = n\omega_{ce}(s_r)$ defines the position s_r, so that

$$\int \alpha_e ds = \sum_{n=1}^{\infty} n_e(s_r) \left[\frac{k T_e(s_r)}{2mc^2}\right]^{n-1} \frac{n^{2n-2}}{(n-1)!} \left(\frac{\pi e R_0}{2\epsilon_0 B_0 c}\right), \quad (2)$$

while $\alpha_o = 0$. The values of $\int \alpha_e ds$ for the CLEO tokamak are listed in Table I together with $1 - r(\omega)$ for stainless steel. We note that harmonics $n < 3$ are optically thick ($\int \alpha_e ds \gg 1 - r$), harmonics $n > 3$ are optically thin ($\int \alpha_e ds \ll 1 - r$), while harmonic $n = 3$ is intermediate, and that T_e can be determined from the ratio of any two harmonics provided they are not both optically thick.

The spectral widths of the various harmonics are determined by the toroidal inhomogeneity of the field, which gives an overlap of harmonics $n = 3$ and 4. However, provided the profiles of $n_e(s)$ and $T_e(s)$ are not particularly flat, the main emission peaks can be calculated separately.

TABLE I. $\int \alpha_e ds$ for the CLEO tokamak and $1 - r(\omega)$ for stainless steel.

n	$\int \alpha_e ds$	$1 - r(\omega)$
2	1.00	5.46×10^{-3}
3	2.96×10^{-3}	6.69×10^{-3}
4	1.46×10^{-5}	7.72×10^{-3}

Figure 2 shows the predictions of this model for the parameters of the CLEO tokamak with the measured parabolic $n_e(s)$, assuming a parabolic $T_e(s)$. Under low-runaway conditions (Fig. 2, curves *a* and *b*) we find that (i) the measured absolute magnitudes exceed the predictions by more than the estimated factor-of-3 uncertainty; (ii) the measured ratios, I_3/I_2 and I_4/I_2, of the intensities of the harmonics yield the electron temperatures 280 eV and 1.1 keV, respectively; and (iii) the main discrepancy is the observed absence of polarization.

Theory for unpolarized emission.—We now assume, on the basis of the subsidiary experiment mentioned above, that each reflection produces some scrambling of the polarizations. We define a transfer fraction p between the two polarizations at each reflection. The boundary condition for the reflected intensity I' then becomes

$$I_{(o,e)}' = r[I_{(o,e)} + p(I_{(e,o)} - I_{(o,e)})], \quad (3)$$

and the transport equation with $\alpha_o = 0$ yields a solution

$$I_e = I_B \frac{1 - \exp(-\int \alpha_e ds)}{1 - \hat{r} \exp(-\int \alpha_e ds)}, \quad (4)$$

$$I_o = I_e r p / (1 - r + rp), \quad (5)$$

where

$$\hat{r} = r[1 - p(1 - r)/(1 - r + rp)].$$

From these equations we see that the emission is completely unpolarized, i.e., $I_e = I_o$ for all n, when $1 - r \ll p$; and that for optically thick harmonics the total intensity, $I_o + I_e = 2I_B$, is double that found when $p = 0$, while for optically thin harmonics the total intensity, $I_o + I_e = I_B \int \alpha_e ds / (1 - r)$, is the same as for $p = 0$.

The predictions of this theory are plotted in Fig. 3. The observed absolute magnitude of I_2 exceeds the prediction by a factor 3.4, just outside the estimated uncertainty. The observed ratios of the peaks yield predicted electron temperatures of 400 eV (I_3/I_2) and 1.4 keV (I_4/I_2). Even allowing for the calibration uncertainty, the discrepancy in I_4 is large and we must look for an alternative explanation for this emission, in particular, in terms of runaway phenomena.

Emission with runaway electrons.—In the presence of a longitudinal electric field the electron distribution function contains a high-energy runaway region and a region of isotropic enhancement of the Maxwellian tail at lower energies. For simplicity, we simulate these distortions by

a second Maxwellian distribution with temperature $T_2 \gg T_i$ and density $n_2 \ll n_i$. The above emission formulas are valid for a double Maxwellian velocity distribution provided that, for the nth harmonic,[9] we replace T_e in I_B by $(n_1 T_1^n + n_2 T_2^n)/(n_1 T_1^{n-1} + n_2 T_2^{n-1})$ and $n_e T_e^{n-1}$ in $\int \alpha_e ds$ by $n_1 T_1^{n-1} + n_2 T_2^{n-1}$. The measured ratios I_3/I_2 and I_4/I_2 together with $n_1 = n_e$ and $T_1 = T_{e0}$ determine independent values $T_2 \sim 36(1 + 2\Delta T_e/T_e)$ keV and $n_2 \sim 8 \times 10^{12}(1 - 7\Delta T_e/T_e)$ m^{-3}, where $\Delta T_e/T_e$ is the uncertainty in the measured electron temperature ($\pm 10\%$). Although sensitive to the peak value of T_e (and to the assumed value of $1 - r$), these results are not significantly modified by different profiles of $T_e(s)$.

One important characteristic of the spectrum observed for high-runaway conditions (Fig. 2, curve c) is the dominant broad peak at $\omega \sim 3.3\omega_{ce}$. Overlapping of I_3 and I_4 in the region $3.2 < \omega/\omega_{ce} < 3.6$ could occur for flat profiles $n_2(s)$ and $T_2(s)$. The above values of n_2 and T_2 are consistent with the ratio of this broad peak to I_2.

Discussion.—It is possible, in view of the uncertain absolute calibration, to assume that the second harmonic in Fig. 3 is fitted by the predicted curve for unpolarized emission [i.e., $2I_B(\omega)$] for the measured $T_e \sim 300$ eV. This change of calibration implies that the fundamental emission should be above the limit of detectability. However, the extraordinary-mode fundamental would be reflected in the decreasing B_φ at the upper-hybrid region,[10,11] leaving the ordinary mode below detectability, consistent with observation.

On the other hand, if I_2 really is well above $2I_B$ (Fig. 3) then we have to explain the suprathermal emission even for $n = 2$.

The main implications of this work are that (i) diagnostic applications may be confused by runaway phenomena, and (ii) the power balance of a fusion reactor may be adversely affected by the enhanced cyclotron emission arising from the depolarization and the runaway effects.

We wish to acknowledge discussions with Dr. D. D. Burgess, Dr. R. J. Bickerton, and E. Puplett and assistance from the CLEO tokamak team and J. Weaver.

*Present address: Division of Electrical Sciences, National Physical Laboratory, Teddington, Middlesex, United Kingdom.

[1]B. A. Trubnikov and A. E. Bazhanova, in *Plasma Physics and the Problems of Controlled Thermonuclear Reactions*, edited by M. A. Leontovich and J. Turkevich (Pergamon, New York, 1959), Vol. 3, p. 141.

[2]M. N. Rosenbluth, Nucl. Fusion 10, 340 (1970).

[3]F. Engelmann and M. Curatolo, Nucl. Fusion 13, 497 (1973).

[4]J. W. M. Paul *et al.*, in *Proceedings of the Sixth European Conference on Controlled Fusion and Plasma Physics, Moscow, 1973* (U.S.S.R. Academy of Sciences, Moscow, 1973).

[5]D. H. Martin and E. Puplett, Infrared Phys. 10, 105 (1970).

[6]A. H. Lichtenberg and S. Sesnic, J. Opt. Soc. Amer. 56, 75 (1966).

[7]Strictly, spectral radiance is in units W m^{-2} sr^{-1} rad^{-1} sec.

[8]G. Bekefi, *Radiation Processes in a Plasma* (Wiley, New York, 1966), p. 41.

[9]G. Bekefi, J. L. Hirshfield, and S. C. Brown Phys. Fluid 4, 173 (1961).

[10]H. Dreicer, in *Plasma Waves in Space and the Laboratory*, edited by J. O. Thomas and B. Landmark (Elsevier, New York, 1969).

[11]A. N. Dellis, private communication.

Rayleigh-Taylor Instability and Laser-Pellet Fusion

Stephen E. Bodner*
Lawrence Livermore Laboratory, Livermore, California 94550
(Received 2 May 1974)

The Rayleigh-Taylor instability in laser-driven spherical implosions can be stabilized by convective flow and by the "fire-polishing" effect, but the size of the stabilization effect depends on details of the thermal conductivity near the ablation surface.

In the basic concept for laser-pellet fusion, a dense cold shell of compressed deuterium-tritium is accelerated radially inward, while being compressed in a nearly adiabatic fashion.[1] When the shell reaches the center, it heats, ignites, and produces thermonuclear burning. The dense shell accelerates inward because of a sharp temperature front that continually ablates the outer

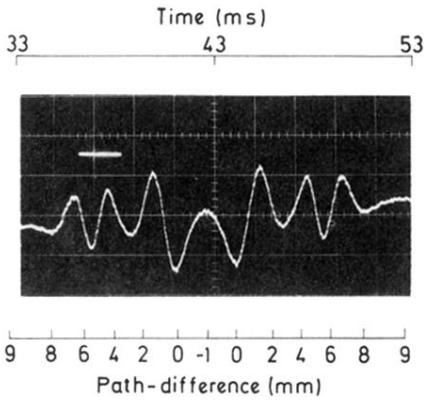

FIG. 1. Signal from the interferometer showing two scans of the interference pattern, traversed in opposite directions. (Time is from initiation of discharge.)